

Synthesis, crystal structure and anticancer activity of the dibutyltin(IV)oxide complexes containing substituted salicylaldehyde-*o*-aminophenol Schiff base with appended donor functionality

Zhi-Jian Zhang, Hui-Ting Zeng, Yang Liu, Dai-Zhi Kuang, Fu-Xing Zhang, Yu-Xing Tan & Wu-Jiu Jiang

To cite this article: Zhi-Jian Zhang, Hui-Ting Zeng, Yang Liu, Dai-Zhi Kuang, Fu-Xing Zhang, Yu-Xing Tan & Wu-Jiu Jiang (2019): Synthesis, crystal structure and anticancer activity of the dibutyltin(IV)oxide complexes containing substituted salicylaldehyde-*o*-aminophenol Schiff base with appended donor functionality, Inorganic and Nano-Metal Chemistry, DOI: [10.1080/24701556.2019.1571513](https://doi.org/10.1080/24701556.2019.1571513)

To link to this article: <https://doi.org/10.1080/24701556.2019.1571513>



Published online: 22 Feb 2019.



Submit your article to this journal [↗](#)



Article views: 7



View Crossmark data [↗](#)



Synthesis, crystal structure and anticancer activity of the dibutyltin(IV)oxide complexes containing substituted salicylaldehyde-*o*-aminophenol Schiff base with appended donor functionality

Zhi-Jian Zhang^a, Hui-Ting Zeng^b, Yang Liu^a, Dai-Zhi Kuang^a, Fu-Xing Zhang^a, Yu-Xing Tan^a, and Wu-Jiu Jiang^a

^aKey Laboratory of Functional Metal-Organic Compounds of Hunan Province Key Laboratory of Functional Organometallic Materials, University of Hunan Province, College of Chemistry and Materials Science, Hengyang Normal University, Hengyang, Hunan, China; ^bHunan Polytechnic of Environment and Biology, School of Medicine Technology, Hengyang, Hunan, China

ABSTRACT

Schiff base butyltin complexes **C1** ~ **C3** have been synthesized *via* the reaction of dibutyltin oxide with the substituted salicylaldehyde-*o*-aminophenol Schiff base ligands (**L1** ~ **L3**), respectively. The complexes have been characterized by elemental analysis, IR, UV-Vis, ¹H NMR, ¹³C NMR spectra and the crystal structures have been determined by X-ray diffraction. The anticancer activity of the Schiff base ligands **L1** ~ **L3** and complexes **C1** ~ **C3** against five species of cancer cells which are MCF7, Colo205, NCI-H460, HeLa and HepG2 were tested respectively, the tests showed that **C3** exhibited significant anticancer activity for the cancer cells in comparison with other complexes. The interaction between **C3** and calf thymus DNA were studied by fluorescence, UV-Vis and Viscosity experiment, the results show that the interaction of **C3** with calf thymus DNA was intercalation.

ARTICLE HISTORY

Received 10 December 2017
Accepted 2 January 2019

KEYWORDS

organotin; Schiff base;
synthesis; crystal structure;
anticancer activity

Introduction

Since the last century, a large number of organotin Schiff base complexes have been reported.^[1–4] Many organotin Schiff base complexes have attracted wide attention because of their good anticancer,^[5,6] bactericidal,^[7,8] antifungal activities and so on.^[9–11] The salicylaldehyde Schiff bases possess O, N multiple sites, so it is a kind of meaningful biological ligand. Their complexes have a rich variety of coordination modes so that it makes the property diversified. To fully understand the mechanism and explore the potential of organotin Schiff base complexes as anticancer drugs, more experimental data and studies are necessary. However, based on our previous work,^[12–17] a series of the salicylaldehyde-*o*-aminophenol Schiff base with appended donor functionality and their organotin complexes have been synthesized, the mechanism of fluorescence emission of complexes was discussed, the anticancer activity and the its interaction with DNA were tested. In order to explore the structure-activity relationship of Schiff base organotin, we further study the anticancer activity of salicylaldehyde-*o*-aminophenol Schiff base organotin complexes *in vitro*, three kinds of substituted salicylaldehyde-*o*-aminophenol and their butyltin complexes were synthesized and characterized in this paper (see Scheme 1). The inhibitory activity of the complexes on cancer cells (MCF7, Colo205, NCI-H460, HeLa and HepG2) and the human normal cell (HL7702) *in vitro*

was tested. And the interaction between the complex with the strongest anticancer activity and calf thymus DNA were studied by fluorescence, utilization of UV-Vis and Viscosity experiment. It provide theoretical basis for the application of this substance to anticancer drugs.

Experimental

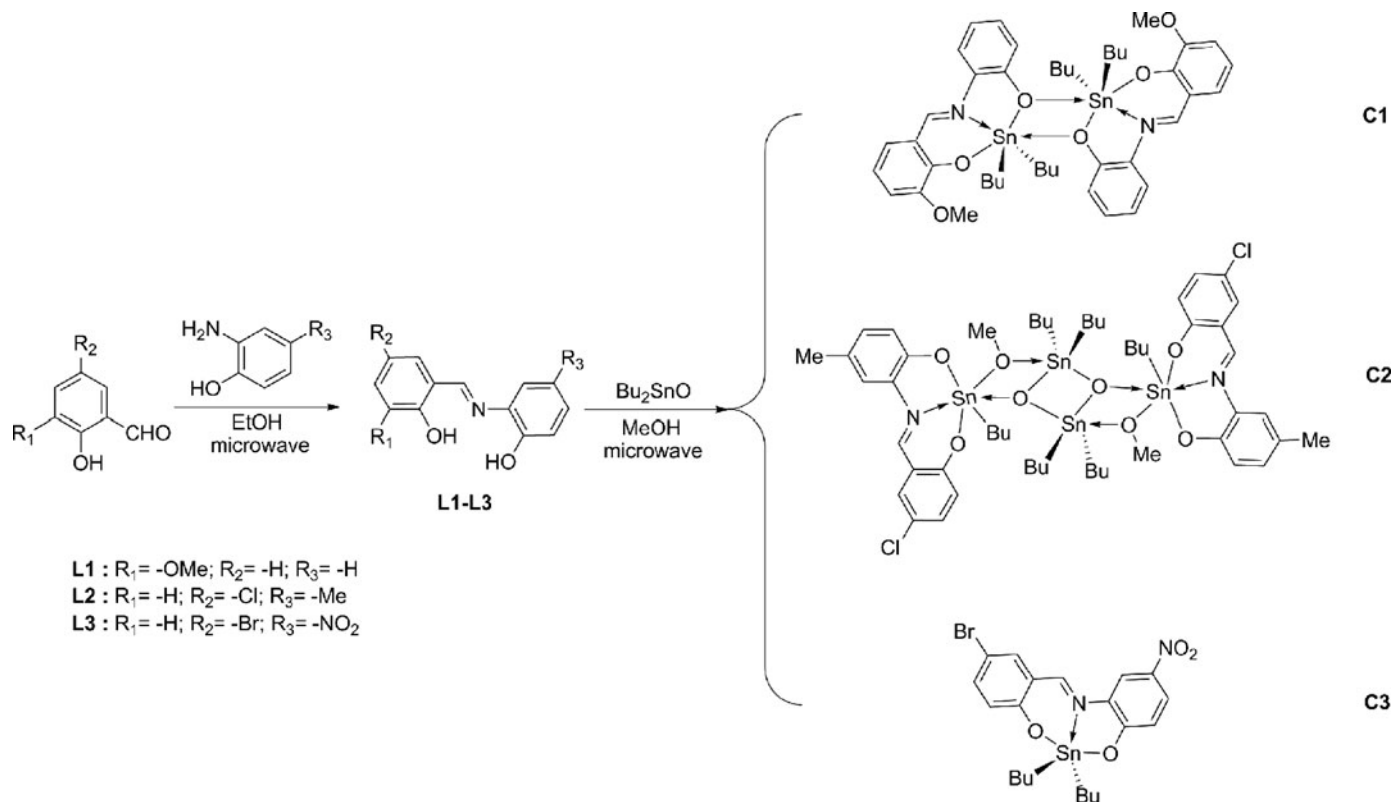
Materials and measurements

All reagents and solvents were available from commercial sources and used as received without further purification. FT-IR spectrum was obtained for KBr pellets on Shimadzu Prestige-21 spectrophotometer in the 4000–400 cm⁻¹. ¹H and ¹³C NMR analysis was performed on a Bruker AVANCE NMR spectrometer. Elemental analyses for C, H, and N were determined on a PE-2400 (II) analyzer. Crystal structure was determined on a CCD area detector X-ray diffractometer. Fluorescence spectra was obtained with a Hitachi F-7000 spectrophotometer with quartz cuvette (path length = 1cm). UV-Vis absorption spectra was measured by UV-2550 spectrometer. Viscosity experiments were conducted on an Ubbelodhe viscometer. Melting point measurement was executed on an X-4 binocular micromelting point apparatus with the temperature unadjusted.

Tris-HCl (0.01 mol·L⁻¹) buffer solution was prepared by a certain amount of Tris dissolved in super pure water

CONTACT Yu-Xing Tan  tanyuxing@hynu.edu.cn Wu-Jiu Jiang  jwj_china@163.com  Key Laboratory of Functional Metal-Organic Compounds of Hunan Province Key Laboratory of Functional Organometallic Materials, University of Hunan Province, College of Chemistry and Materials Science, Hengyang Normal University, Hengyang, Hunan, 421008, China.

Color versions of one or more of the figures in the article can be found online at www.tandfonline.com/lsrt.



Scheme 1. Synthesis of complexes.

before using, the pH of the solution was adjusted to 7.40 with hydrochloric acid solution (0.1 mol·L⁻¹). The purity of calf thymus DNA was determined by comparing the absorbance at 260 and 280 nm ($A_{260}/A_{280} = 1.8 \sim 1.9/1$). The concentration of calf thymus DNA was calculated by measuring the absorbance at 260 nm ($\epsilon_{260} = 6600 \text{ L}\cdot\text{mol}^{-1}\cdot\text{cm}^{-1}$). The reserve liquid was stored at 4 °C. The ethidium bromide solution was prepared by a certain amount of ethidium bromide solid dissolved in Tris-HCl (0.01 mol·L⁻¹) buffer solution.

Synthesis of ligands (L1 ~ L3)

According to literatures,^[12] a mixture of substituted salicylaldehyde (10 mmol), absolute ethanol (20 mL) and substituted *o*-aminophenol (10 mmol) were added to microwave reactor, the reaction continued for about 30 min at 100 °C. After that, the solvent was removed by evaporation in vacuo and the residual solution was filtered. It was recrystallized by absolute ethanol.

3-MeOC₆H₃(OH)C=NC₆H₄(OH) (**L1**): Yield: 84.6%. m.p.: 197–198 °C. Anal. Calc. for (C₁₄H₁₃NO₃): C 69.12, H 5.39, N 5.76%. Found: C 69.15, H 5.38, N 5.75%. IR (KBr, cm⁻¹): 3500(w), 3047 (w), 2988 (w), 1627 (s), 1539 (m), 1508 (s), 1244(s), 1168 (s), 1029 (m), 740 (s). ¹H NMR (CDCl₃, 400 MHz, δ /ppm): 12.51 (s, 1H), 8.71 (s, 1H), 7.17–7.26 (m, 2H), 7.02–7.09 (m, 3H), 6.91–6.99 (m, 2H), 5.87 (s, 1H), 3.94 (s, 3H).

5-ClC₆H₃(OH)C=NC₆H₃(OH)-4-Me (**L2**): Yield: 75.9%. m.p.: 175–176 °C. Anal. Calc. for (C₁₄H₁₂ClNO₂): C 64.25, H 4.62, N 5.35%. Found: C 64.26, H 4.62, N 5.34%. IR

(KBr, cm⁻¹): 3445 (w), 3086 (w), 2945 (w), 1627 (s), 1519 (s), 1395 (s), 1251 (s), 1032 (m), 797 (s). ¹H NMR (CDCl₃, 400 MHz, δ /ppm): 12.41 (s, 1H), 8.61 (s, 1H), 7.33–7.40 (m, 2H), 6.90–7.05 (m, 4H), 5.56 (s, 1H), 2.33 (s, 3H).

5-BrC₆H₃(OH)C=NC₆H₃(OH)-4-NO₂ (**L3**): Yield: 77.6%. m.p.: 300–301 °C. Anal. Calc. for (C₁₃H₉BrN₂O₄): C 46.32, H 2.69, N 8.31%. Found: C 49.30, H 2.70, N 8.31%. IR (KBr, cm⁻¹): 3454 (w), 3077 (w), 1619 (s), 1512 (w), 1375 (s), 1288 (s), 1033 (m), 742 (m). ¹H NMR (CDCl₃, 400 MHz, δ /ppm): 13.15 (s, 1H), 11.43 (s, 1H), 9.14 (s, 1H), 8.14 (d, $J = 8.8$ Hz, 1H), 8.13 (s, 1H), 8.00 (s, 1H), 7.62 (d, $J = 8.4$ Hz, 1H), 7.17 (d, $J = 8.8$ Hz, 1H), 7.00 (d, $J = 8.8$ Hz, 1H).

Synthesis of complexes (C1 ~ C3)

A mixture of dibutyltin oxide (1 mmol), absolute methanol (20 mL) and Schiff base ligands (**L1**, **L2** or **L3**) (1 mmol) were added to microwave reactor, respectively. The reaction continued for about 30 min at 120 °C. After that, the solvent was removed by evaporation in vacuo and the residual solution was filtered, and the solids were recrystallized by absolute methanol.

{[3-MeOC₆H₃(O)C=NC₆H₄(O)]*n*-Bu₂Sn}₂ (**C1**): The product was red-brown crystal, Yield: 73.9%. m.p.: 138 ~ 140 °C. Anal. Calc. (C₂₂H₂₉NO₃Sn): C 55.73, H 6.16, N 2.95%. Found: C 55.75, H 6.15, N 2.94%. IR (KBr, cm⁻¹): 3060 (w), 3025 (w), 2953(m), 2920(m), 1602 (s), 1584 (s), 1541(m), 1480 (s), 1225 (s), 1149 (s), 745 (s), 565 (m), 522 (w), 469(w), 419 (w). ¹H NMR(CDCl₃, 400 MHz, δ /ppm): 8.66, (s, 1H), 7.34 (d, $J = 7.9$ Hz, 1H), 7.17 (t, $J = 7.6$ Hz,

Table 1. Crystallographic data of the complexes.

Complex	C1	C2	C3
Empirical formula	C ₂₂ H ₂₉ NO ₃ Sn	C ₅₄ H ₈₀ Cl ₂ N ₂ O ₈ Sn ₄	C ₂₁ H ₂₅ BrN ₂ O ₄ Sn
Mr	474.15	1430.86	568.03
Temperature / K	296(2)	296(2)	296(2)
Crystal system	Monoclinic	Triclinic	Monoclinic
Space group	<i>P</i> 2 ₁ / <i>n</i>	<i>P</i> $\bar{1}$	<i>P</i> 2 ₁ / <i>c</i>
<i>a</i> / Å	12.4970(4)	11.3731(9)	17.1353(9)
<i>b</i> / Å	17.9750(6)	11.7547(10)	9.5197(5)
<i>c</i> / Å	19.3207(6)	12.4378(10)	14.3022(7)
α / °	90	100.5200(10)	90
β / °	98.994(2)	100.5330(10)	96.7560(10)
γ / °	90	107.6200(10)	90
Volume / Å ³	4286.7(2)	1507.0(2)	2316.8(2)
Z	8	1	4
<i>D</i> _c / Mg/m ³	1.469	1.577	1.629
Absorption coefficient / mm ⁻¹	1.213	1.776	2.855
<i>F</i> (000)	1936	716	1128
Crystal size / mm	0.35 × 0.23 × 0.21	0.21 × 0.19 × 0.18	0.23 × 0.21 × 0.18
θ range / (°)	1.82 ~ 25.10	2.77 ~ 25.10	2.45 ~ 25.10
Limiting indices	-14 ≤ <i>h</i> ≤ 14, -21 ≤ <i>k</i> ≤ 21, -22 ≤ <i>l</i> ≤ 23	-13 ≤ <i>h</i> ≤ 13, -14 ≤ <i>k</i> ≤ 14, -14 ≤ <i>l</i> ≤ 14	-20 ≤ <i>h</i> ≤ 20, -11 ≤ <i>k</i> ≤ 5, -17 ≤ <i>l</i> ≤ 17
Reflections collected / unique	23656 / 7628 [<i>R</i> _{int} = 0.0175]	15586 / 5338 [<i>R</i> _{int} = 0.0231]	12448 / 4132 [<i>R</i> _{int} = 0.0187]
Completeness	99.9 %	99.5 %	100.0 %
Max. and min. transmission	0.7848 and 0.6762	0.7405 and 0.7067	0.6275 and 0.5597
Data / restraints / parameters	7628 / 14 / 564	5338 / 69 / 394	4132 / 20 / 281
Goodness-of-fit on <i>F</i> ²	1.031	1.079	1.025
Final <i>R</i> indices [<i>I</i> > 2 σ (<i>I</i>)]	<i>R</i> ₁ = 0.0263, <i>wR</i> ₂ = 0.0632	<i>R</i> ₁ = 0.0409, <i>wR</i> ₂ = 0.1225	<i>R</i> ₁ = 0.0314, <i>wR</i> ₂ = 0.0763
<i>R</i> indices (all data)	<i>R</i> ₁ = 0.0323, <i>wR</i> ₂ = 0.0659	<i>R</i> ₁ = 0.0626, <i>wR</i> ₂ = 0.1341	<i>R</i> ₁ = 0.0565, <i>wR</i> ₂ = 0.0833
$\Delta\rho_{\max}$ and $\Delta\rho_{\min}$ (e. Å ⁻³)	0.663 and -0.558	0.708 and -0.588	0.393 and -0.231

1H), 6.95 (d, *J* = 7.9 Hz, 1H), 6.84–6.89 (m, 2H), 6.65–6.71 (m, 2H), 3.86 (s, 3H), 1.52–1.62 (m, 8H), 1.26–1.35 (sext, *J* = 7.3 Hz, 4H), 0.82 (t, *J* = 7.3 Hz, 6H). ¹³C NMR (CDCl₃, 100 MHz, δ /ppm): 161.81, 160.63, 159.72, 151.78, 131.79, 130.00, 126.60, 118.54, 117.83, 116.93, 116.19, 115.96, 114.75, 56.36, 26.95, 26.53, 22.28, 13.47.

(μ_3 -O)₂(μ_2 -OCH₃)₂[5-ClC₆H₃(O)C = NC₆H₃(O)-4-Me]₂(*n*-BuSn)₂(*n*-Bu₂Sn)₂ (**C2**): The product was red-brown crystal, Yield: 72.8%. m.p.: 130 ~ 133 °C. Anal. Calc. (C₅₄H₈₀Cl₂N₂O₈Sn₄): C 45.33, H 5.64, N 1.96%. Found: C 45.30, H 5.64, N 1.95%. IR (KBr, cm⁻¹): 3040 (w), 3025 (w), 2953(m), 2920(m), 1604 (s), 1523 (s), 1490(s), 1458 (s), 1261 (s), 1165 (s), 765 (s), 607(m), 557 (m), 476 (w), 408 (w). ¹H NMR(CDCl₃, 400 MHz, δ /ppm): 8.39 (s, 1H), 7.20–7.23 (m, 2H), 7.14(s, 1H), 7.00 (d, *J* = 7.3 Hz, 1H), 6.75–6.79 (m, 2H), 2.29 (s, 3H), 1.26–1.32 (m, 10H), 1.13–1.14 (m, 4H), 0.89–0.92 (m, 10H), 0.70 (t, *J* = 7.0 Hz, 3H). ¹³C NMR (CDCl₃, 100 MHz, δ /ppm): 159.70, 136.19, 134.86, 133.23, 133.04, 131.52, 125.81, 124.46, 124.09, 120.94, 119.59, 118.50, 114.97, 50.45, 27.59, 27.01, 26.61, 26.45, 22.13, 20.78, 20.72, 13.72, 13.50.

[5-BrC₆H₃(O)C = NC₆H₃(O)-4-NO₂]*n*-Bu₂Sn (**C3**): The product was orange crystal, Yield: 75.5%. m.p.: 120 ~ 123 °C. Anal. Calc. (C₂₁H₂₅BrN₂O₄Sn): C 44.40, H 4.44, N 4.93%. Found: C 44.41, H 4.44, N 4.94%. IR (KBr, cm⁻¹): 3053 (w), 2955 (w), 29894 (w), 1604 (s), 1519 (s), 1490 (s), 1316 (s), 1302(s), 1157(s), 648 (m), 580 (w), 511 (w), 472 (m), 418 (m). ¹H NMR(DMSO-*d*₆, 400 MHz, δ /ppm): 9.26 (s, 1H), 8.63 (s, 1H), 8.04 (d, *J* = 7.9 Hz, 1H), 7.84 (s, 1H), 7.49 (d, *J* = 7.9 Hz, 1H), 6.78 (d, *J* = 8.8 Hz, 1H), 6.95 (d, *J* = 8.8 Hz, 1H), 1.36–1.43 (m, 8H), 1.17–1.22 (m, 4H), 0.73 (t, *J* = 7.0 Hz, 3H). ¹³C NMR (DMSO-*d*₆, 100 MHz, δ /ppm): 168.00, 166.45, 164.50, 138.82, 137.74, 135.98, 131.89,

125.38, 123.97, 119.65, 117.51, 113.07, 105.91, 26.53, 25.50, 25.13, 13.17.

X-ray crystallography diffraction

X-ray diffraction data for crystals were performed with graphite monochromated Mo-*K*_α radiation (λ = 0.71073 Å) on a Bruker Smart Apex II CCD diffractometer, and collected by the $\varphi \sim \omega$ scan technique at ambient temperature. Multi-scan absorption correction was applied to the data. The crystal structures were solved by direct methods and refined by full-matrix least-squares on *F*². All the non-hydrogen atoms were located in successive difference Fourier syntheses and then refined anisotropically. Hydrogen atoms were placed in calculated positions or located from the Fourier maps, and refined isotropically with the isotropic vibration parameters related to the non-hydrogen atom to which they are bonded. All calculations were performed with SHELXL-97 programs within WINGX.^[18,19] The crystal data and structure refinement parameters of complexes are listed in Table 1.

UV-Vis property

The solutions of **C1** ~ **C3** were prepared with acetone at room temperature, respectively, and their concentration was 1 × 10⁻⁵ mol/L. The scan range is from 340 to 600 nm, and the width of slit scanning is 5.0 nm.

Anticancer activity studies

Primary human liver HL-7702 cells were purchased from institute of Biochemistry and Cell Biology, Chinese

Academic of science. MCF7, Colo205, NCI-H460, HeLa and HepG2 cells were obtained from American Tissue Culture Collection (ATCC). HL-7702 cells were cultured in Dulbecco's modified Eagle's medium (Thermo Fischer Scientific) containing 4500 mg/L glucose, supplemented with 10% fetal bovine serum (GIBICO, Invitrogen) and *L*-glutamine. The other cells were maintained at 37 °C in a 5% CO₂ incubator in RPMI 1640 (GIBICO, Invitrogen) containing 10% fetal bovine serum (GIBICO, Invitrogen). The test drug was added from a stock solution in DMSO to result in a final DMSO concentration of less than 0.1%. Cell proliferation was assessed by MTT assay. The cells were exposed to treatment for 24 hrs, and the number of cells used per experiment for each cell line was adjusted to obtain an absorbance at 570 nm. Six concentrations (0.1 nM–10 μM) were set for the compounds and at least 3 parallels of every concentration were used. All experiments were repeated at least three times. The data was calculated using Graph Pad Prism version 7.0. The IC₅₀ were fitted using a non-linear regression model with a sigmoidal dose response.

Interaction with DNA studies

A mixture of the thymus DNA, EB and complex solution of different concentration was placed in a 5 mL volumetric flask. After 3 h, the fluorescence spectra were scanned at 25 °C respectively, the emission wavelength was 258 nm, and the excitation wavelength was shown in the spectrum. The emission and excitation slit scanning width was 5.0 nm.

In order to accurately express the strength of the interaction between the complex and the DNA, the binding constant (K_b) can be obtained according to the following formula:^[20]

$$c_{\text{DNA}}/(\varepsilon_A - \varepsilon_F) = c_{\text{DNA}}/(\varepsilon_B - \varepsilon_F) + 1/K_b(\varepsilon_B - \varepsilon_F)$$

where c_{DNA} is the concentration of CT-DNA, ε_A is the observed extinction coefficient at arbitrary DNA concentration, ε_F is the extinction coefficient of the free complex, ε_B is the extinction coefficient of the complex when fully combine to CT-DNA. Data was presented as $c_{\text{DNA}}/(\varepsilon_A - \varepsilon_F)$ versus c_{DNA} , and the ratio of the slope to the intercept is the binding constant (K_b). The mixture of the complex (50 μM) and different concentration CT-DNA (0–50 μM) was added in a 5 mL volumetric flask. After 3 hrs, the absorption spectra were scanned at 25 °C, respectively.

The viscosity tests were executed in the Ubbelodhe viscometer, and it was keep in the 25.0 ± 0.1 °C with water bath. The different concentration complex (0–50 μM) and CT-DNA solution (50 μM) were added in the viscometer, respectively. The values of viscosity were calculated from the flow times of CT-DNA containing solutions corrected for the flow time of buffer alone (t_0), $\eta = (t - t_0)^{[21]}$ Data was presented as $(\eta/\eta_0)^{1/3}$ versus $(c_{\text{complex}}/c_{\text{DNA}})$, where η is the viscosity of CT-DNA in the presence of the complex, η_0 is the viscosity of CT-DNA alone, c_{complex} is the concentration of the complex and c_{DNA} is the concentration of CT-DNA.

Results and discussion

FT-IR spectra

Since all absorption peaks follow the same pattern, we present the data of **L1** and **C1** as examples. In contrast to the FT-IR spectra of **L1** and **C1**, the presence of a single band in the 3500 cm⁻¹ (**L1**) was assigned to phenolic hydroxyl, but this peak disappears in the **C1**, it indicated that the phenolic hydroxyl group have lost hydrogen protons to coordinate with the dibutyltin oxide. Besides, a series of new absorption peak appeared in the low frequency region, the absorption bands at the 522 cm⁻¹ and 469 cm⁻¹ correspond to the $\nu(\text{Sn-O})$ and $\nu(\text{Sn-N})$,^[22,23] respectively. There is a good indication of complex formation.

To summarize, the FT-IR spectra of ligands (**L1** ~ **L3**) show broad bands at 3445–3500 cm⁻¹ assignable to $\nu(\text{OH})$,^[6] and this peak disappears after coordinating. Characteristic bands at 1508–1541 cm⁻¹ are assigned to stretching vibration of the $\nu(\text{C=N})$.^[24,25] The bands at 1149–1288 cm⁻¹ are assigned to the $\nu(\text{C-O})$.^[26] Some new bands in the ranges from 511 to 557 cm⁻¹ and 469 to 478 cm⁻¹ which appeared in the spectra of the synthesized metal complex were probably due to (Sn–O) and (Sn–N) bond vibration frequencies.^[23, 27]

NMR spectra

The ¹H NMR spectrum show the ratio of the integral area of each group is consistent with the expected number of protons in each group.^[28,29] Two phenolic hydroxy peaks at 12.41–13.15 and 8.61–11.43 ppm of the ligand disappeared in the complex, and the hydrogen absorption peaks of butyl groups were found in the high field, thus it can reasonably be assumed that the Schiff bases ligand have bonded with organotin.

In the ¹³C NMR spectrum of **C1** ~ **C3**, the absorption peaks of carbon linked to nitrogen was at 161.81, 159.70, 168.00 ppm,^[30] respectively. The peak positions of all carbon atoms were basically consistent with the theoretical prediction structure. And the conclusions are supported by the results of X-ray diffraction studies.

Description of the structures

The structures of **C1** ~ **C3** are illustrated in Figures 1–3. Selected bond distances and angle are list in Table 2. From the Figure 1, it can be seem that there are two independent dinuclear molecule. The coordinated environment of their central tin atom is similar. In an independent molecule containing Sn^I and Sn^{II}, a Sn₂O₂ planar four-membered ring was constituted through Sn^I, Sn^{II} bridging the two phenol oxygen atoms O² and O²ⁱⁱ. The center of the Sn₂O₂ ring is the symmetry center of this independent molecule. The distance of Sn^I–O² is 2.126 Å and the Sn^I–O²ⁱⁱ is 2.862 Å, it has subtle difference with the literature.^[31,32] The central tin atom is six-coordinate octahedral geometry, the O¹, O², N¹ and O²ⁱⁱ were placed in equatorial sites, the axis position were occupied by two carbon (C¹⁵ and C¹⁹) from butyl

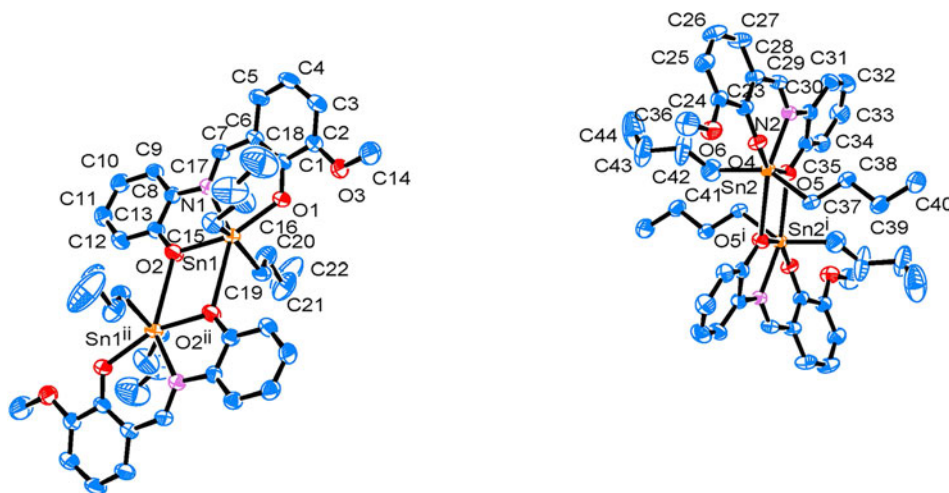


Figure 1. Molecular structure of C1. (Symmetry codes: ⁱ 1-x, 2-y, 2-z; ⁱⁱ 1-x, 1-y, -z).

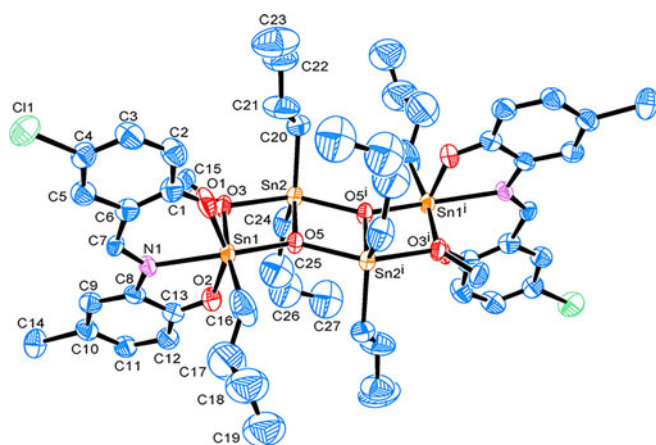


Figure 2. Molecular structure of C2. (Symmetry code: ⁱ -x+1, -y+1, -z+1).

group. The angles [C19-Sn1-O2ⁱⁱ 75.90°, C19-Sn1-O2 97.75°, C19-Sn1-N1 109.47°, C19-Sn1-O1 87.81°, C15-Sn1-O2ⁱⁱ 79.59°, C15-Sn1-O2 92.1°, C15-Sn1-N1 103.0°, C15-Sn1-O1 95.8°] are obviously deviated from 90°, and the angle of C15-Sn1-C19 is 147.5°, which are also deviated from linear angle 180°. In addition, the angle of four atoms at the equatorial sites [O1-Sn1-O2ⁱⁱ 136.70°, O1-Sn1-N1 80.88°, O2ⁱⁱ-Sn1-O2 67.37°, O2-Sn1-N1 74.96°] are greatly deviated from 90°. Above description indicated that the central tin atom is six-coordinate in distorted octahedron geometry. The coordination environment of Sn1ⁱⁱ, Sn2 and Sn2ⁱ is consistent with Sn1.

The ladder structure of C2 was constituted by three Sn₂O₂ four-membered rings, and the three four-membered rings are coplanar. In this ladder structure, the geometries of all the tin atoms can be classified into two types, the first type of tin atom (Sn1) is six-coordinate geometry, and it occupied the top of the ladder. Besides, the de-alkylation reaction have occurred,^[33] and one butyl was laid off on the Sn1. It can be seen that the Sn1 is surrounded by two oxygen atoms (O1 and O2) and one nitrogen atom (N1) from the ligand, one carbon atom (C16) from butyl, one oxygen atoms (O3) from methanol molecule and one μ-O atom. The second type of tin (Sn2) located in the middle of the ladder, it is five-coordinate geometry, and this kind of

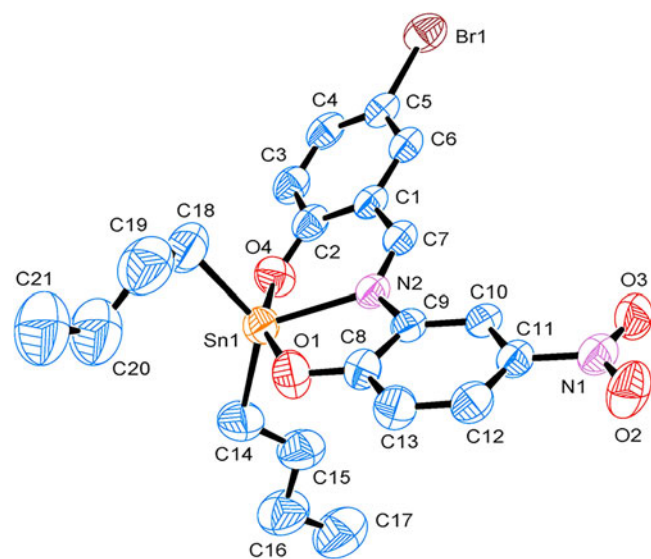


Figure 3. Molecular structure of C3.

tin atom and μ-O atom connected Sn₂O₂ four-membered rings, respectively. Thus it made C2 present a ladder structure. The Sn2 is surrounded by two carbon atoms (C20 and C24) from the two different butyl, one oxygen atoms (O3) from methanol molecule and two μ-O atoms. The four-membered ring in the middle can be viewed as the center of molecule.

For the structure of C3, it is a monomer structure, the central tin atom is five-coordinate in distorted trigonalbipyramid geometry, it is similar to the complex.^[34,35] In the crystal of C3, there are rich intermolecular hydrogen bonding interaction. The dimer structure was formed by O-H...O hydrogen bonds (H6...O2ⁱ 2.427Å, ∠O6-H6...O2ⁱ 176.55°; H7...O3ⁱ 2.651Å, ∠O7-H7...O3ⁱ 163.02°; H10...O3ⁱ 2.672Å, ∠O10-H10...O3ⁱ 127.58°; i: 2-x, 2-y, 1-z) (Figure 4).

UV-Vis

The UV-Vis absorption spectra of C1 ~ C3 were shown in Figure 5. It is obvious that the C1 ~ C3 have a large

Table 2. Parts of bond lengths (Å) and bond angles (°) of **C1** ~ **C3**.

C1					
Bond					
Sn1–C19	2.116(3)	Sn2–O5	2.124(2)	Sn1–O1	2.146(2)
Sn1–C15	2.148(19)	Sn2–C41	2.07(3)	Sn1–O2	2.126(2)
Sn1–N1	2.225(2)	Sn2–O4	2.1762(19)	Sn1–O2 ⁱⁱ	2.862(2)
Sn2–C37	2.119(3)	Sn2–N2	2.215(2)	Sn2–O5 ⁱ	2.866(2)
Angle					
C19–Sn1–O2	97.75(11)	C41–Sn2–C37	142.8(10)	C19–Sn1–O1	87.81(11)
C19–Sn1–N1	109.47(12)	C41–Sn2–N2	107.1(10)	O1–Sn1–N1	80.88(8)
C19–Sn1–C15	147.5(4)	C41–Sn2–O5	96.4(8)	O2–Sn1–O1	155.70(8)
O2–Sn1–N1	74.96(8)	C37–Sn2–N2	109.64(10)	O2–Sn1–C15	92.1(4)
C15–Sn1–O1	95.8(5)	O5–Sn2–O4	155.09(7)	C15–Sn1–N1	103.0(4)
C19–Sn1–O2 ⁱⁱ	75.905(91)	C37–Sn2–O5 ⁱ	76.722(81)	C15–Sn1–O2 ⁱⁱ	79.591(514)
C41–Sn2–O4	92.3(8)	C37–Sn2–O4	88.45(10)	O5–Sn2–N2	75.26(8)
O4–Sn2–N2	79.88(8)	C37–Sn2–O5	98.33(10)	C41–Sn2–O5 ⁱ	78.942(702)
C2					
Bond					
Sn1–O1	1.889(9)	Sn2–O5	2.027(3)	Sn1–O3	2.090(3)
Sn1–N1	2.298(5)	Sn2–C20	2.113(6)	Sn1–O2	2.040(11)
Sn1–O5	2.029(3)	Sn2–O5 ⁱ	2.127(5)	Sn1–C16	2.152(6)
Sn2–C24	2.121(5)	Sn2–O3	2.170(3)		
Angle					
O1–Sn1–O5	110.0(3)	O1–Sn1–N1	84.4(3)	O1–Sn1–O3	86.5(3)
O1–Sn1–C16	97.8(4)	O5–Sn2–C24	117.1(2)	O3–Sn1–C16	171.6(2)
O2–Sn1–N1	64.6(3)	C20–Sn2–O3	96.72(18)	O5–Sn1–O2	96.1(3)
O2–Sn1–O3	82.1(3)	C24–Sn2–O5 ⁱ	98.90(19)	O2–Sn1–C16	97.7(4)
O5–Sn1–N1	154.36(14)	O5–Sn2–C20	117.73(19)	C16–Sn1–N1	101.8(2)
O1–Sn1–O2	147.6(4)	O5–Sn2–O3	72.82(11)	O5–Sn1–O3	74.49(12)
O5–Sn1–C16	97.2(2)	O3–Sn1–N1	85.74(15)	C20–Sn2–O5 ⁱ	98.6(2)
C20–Sn2–C24	125.0(3)	O5–Sn2–O5 ⁱ	75.33(11)	O5 ⁱ –Sn2–O3	148.14(12)
C24–Sn2–O3	94.8(2)				
C3					
Bond					
Sn1–O4	2.087(3)	Sn1–C18	2.111(5)	Sn1–O1	2.122(3)
Sn1–C14	2.120(4)	Sn1–N2	2.197(3)		
Angle					
O4–Sn1–C18	95.08(19)	O4–Sn1–C14	90.56(17)	O4–Sn1–O1	157.49(11)
O4–Sn1–N2	82.46(11)	C18–Sn1–N2	111.59(16)	O1–Sn1–N2	75.69(10)
C18–Sn1–C14	128.9(2)	C14–Sn1–N2	119.46(15)	C18–Sn1–O1	97.89(19)
C14–Sn1–O1	95.45(17)				

absorption at about 460 nm, the reason for this may be that the nitrogen atoms on the ligands are coordinated with tin, and the electrons transfer from the ligand to the Sn atom, the C=N bond polarized so that the energy of the related conjugated molecular orbital were affected.^[12, 36] It further confirmed that Schiff base ligand have coordinated dibutyltin oxide, and the Schiff base organotin(IV) complexes were synthesized. Besides, as can be seen from the Figure 5, a absorption were presented at about 350 nm for **C3**, it may be surmised that the transition of $n \rightarrow \pi^*$ on the nitro group have occurred, and the nitro is a chromophoric group so that it has a slight red shift.^[37]

Anticancer activity

Table 3 lists the half inhibitory concentration of the complexes and carboplatin on cultured cancer cells (MCF7, Colo205, NCI-H460, Hela, HepG2) and the human normal cell (HL7702) in vitro. In the toxicity test for HL7702, it have found that all Schiff base ligands are relatively low-toxic for the human normal cell HL7702, the activity decreased in the following order: **L2** > **L3** > **L1**, which corresponds to IC₅₀ value at 22.36, 24.23, and 34.15 μ M respectively, and the toxicity activity of complexes (**C1** ~ **C3**) are greater than the corresponding Schiff base ligands.

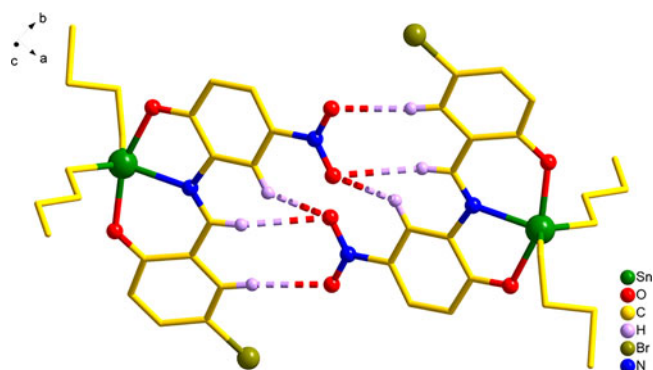


Figure 4. The dimer structure of **C3** constructed by intermolecular hydrogen bonding.

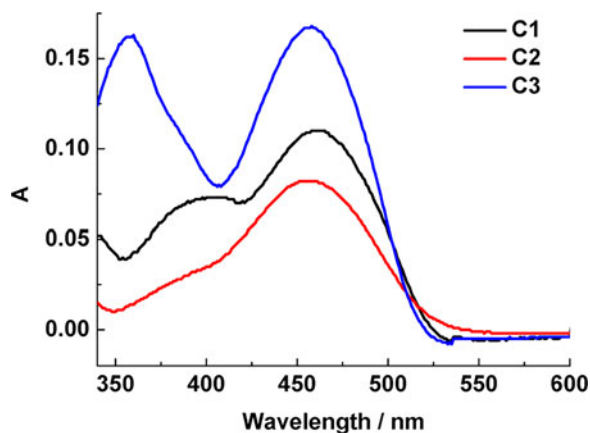


Figure 5. UV-Vis spectrum of the complexes.

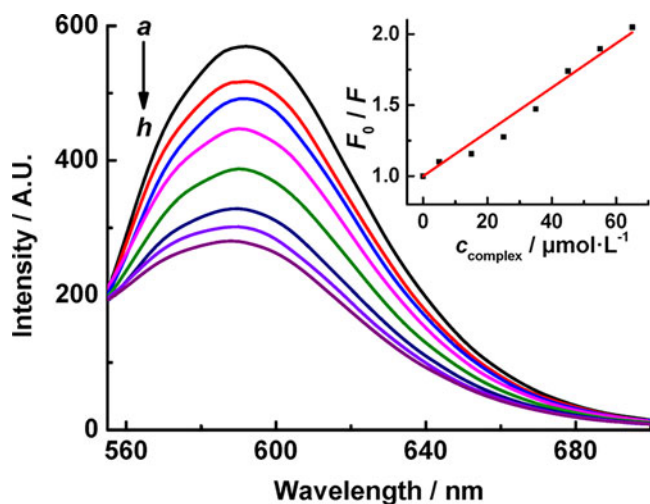
Also, it have discovered that the organotin Schiff base complexes (**C1** ~ **C3**) exhibited better anticancer activity for the five kinds of cancer cells in comparison with the Schiff base ligand, and some of these compounds has greater effect than carboplatin on the specified cancer cell. Especially, the effect of **C3** on Hela cancer cells is stronger than carboplatin and other complexes, So **C3** may become candidate compound for treatment of cervical cancer after further chemical optimization. From the structure of the complexes, it can be found that **C1** ~ **C3** are butyl tin compounds, but the substituents on the Schiff base are different. The difference activity of complexes may be caused only by a substituent on the Schiff base ligand, it can infer that ligand has a great influence on the anticancer activity of complexes from Table 3, especially for compounds containing electron withdrawing group (e.g. $-X$ or $-\text{NO}_2$), the activity of **C3** is obviously better than **C1** and **C2**. In **C3**, the bromine atom and the nitro group on the Schiff base are electron withdrawing groups. Those results suggest that the anticancer activity of the complex is related to the electrical effect of the substituent on the Schiff base ligand.

Interaction with DNA

Ethidium bromide (EB) is a fluorescent dye, but its fluorescence is very weak. In DNA solution, EB can be inserted in the base of double helix DNA in parallel to enhance its fluorescence. Competitive reaction would take place when

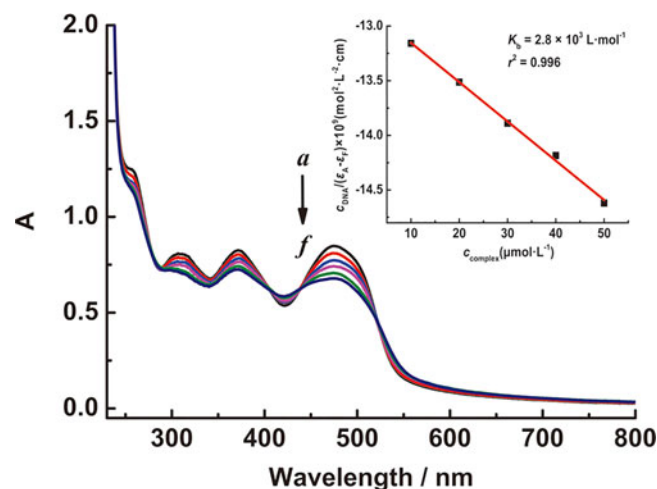
Table 3 Inhibition action of ligands and complexes to cancer cell *in vitro*.

Complex	IC ₅₀ (μM)					
	MCF7	Colo205	NCI-H460	Hela	HepG2	HL7702
L1	23.55 ± 1.07	17.53 ± 1.11	26.62 ± 2.13	17.61 ± 1.39	20.06 ± 0.77	34.15 ± 1.75
L2	17.50 ± 1.46	18.33 ± 1.22	15.18 ± 0.92	10.80 ± 0.50	14.72 ± 1.80	22.36 ± 1.19
L3	16.31 ± 0.70	19.65 ± 1.31	16.00 ± 2.74	11.06 ± 1.60	14.14 ± 0.48	24.23 ± 1.81
C1	7.24 ± 1.34	6.02 ± 0.91	7.86 ± 0.26	9.25 ± 0.44	9.88 ± 0.31	20.29 ± 0.49
C2	9.37 ± 1.05	6.85 ± 0.88	9.25 ± 0.37	8.56 ± 1.24	10.87 ± 0.29	13.41 ± 1.30
C3	5.45 ± 0.47	6.47 ± 0.54	7.25 ± 1.02	3.23 ± 1.74	9.56 ± 1.52	16.85 ± 1.30
Carboplatin	8.22 ± 1.29	3.88 ± 0.61	6.26 ± 1.02	22.56 ± 1.79	1.70 ± 0.32	21.38 ± 2.41

**Figure 6.** Effects of C3 on the fluorescent spectra of EB-DNA system. ($c_{\text{DNA}} = 30 \mu\text{mol}\cdot\text{L}^{-1}$; $c_{\text{EB}} = 3 \mu\text{mol}\cdot\text{L}^{-1}$; from a to h, $c_{\text{complex}} = 0, 10, 20, 30, 40, 50, 60, 70 \mu\text{mol}\cdot\text{L}^{-1}$, respectively; Inset: plot of F_0/F vs c_{complex} ; $\lambda_{\text{ex}} = 258 \text{ nm}$).

the complex was added to the EB-DNA system solution, complex can squeeze EB out of the DNA double helix, resulting in quenching of fluorescence intensity. Thus, EB could be used as a fluorescent probe of DNA structure.^[38] Figure 6 is fluorescence quenching curve of different concentration complex on the EB-DNA system. The fluorescence of EB-DNA system was obviously declined along with increasing the concentration of C3. It indicated that the complex involved in the coordination with the base pairs of DNA and it squeezed EB out of the DNA double helix, so the presence of complex makes the fluorescence of EB-DNA system quenched. From the curve in figure6, it can inferred that the interaction of C3 with DNA was intercalation model and the way of quenching is static quenching. The quenching constant was calculated using the Stern-Volmer equation: $I_0/I = 1 + K_{\text{SV}} \times c_{\text{complex}}$,^[39] the K_{SV} was calculated as $1.56 \times 10^4 \text{ L}\cdot\text{mol}^{-1}$, this value is similar to that reported in the literature.^[27, 40] It indicated that the C3 has a strong intercalation with DNA, and can be assumed that the tin atom of C3 combined the base pairs of DNA, the terminal ligands inserted into the DNA base pairs to compete with EB, so that EB was squeeze out the DNA double helix by C3.

The electronic absorption spectra of C3 in the absence and presence of CT-DNA are shown in Figure 7. With the addition of DNA, the absorbance has decreased, this absorption bands exhibited hypochromism of 20.1%. The hypochromism value reflected the interaction force of complexes with DNA at a certain extent. If the color reduction rate is

**Figure 7.** Electronic spectra of C3 in Tris-HCl buffer upon addition of CT-DNA. ($c_{\text{complex}} = 50 \mu\text{mol}\cdot\text{L}^{-1}$; from a to f, $c_{\text{DNA}} = 0, 10, 20, 30, 40, 50 \mu\text{mol}\cdot\text{L}^{-1}$, respectively. Arrow shows the absorbance changing upon the increase of DNA concentration; Inset: plots of $c_{\text{DNA}}/(\epsilon_A - \epsilon_f)$ vs. c_{DNA}).

less than 10%, it is considered that the complex has a weak interaction with DNA. The higher the color reduction rate, the stronger the interaction between the complex and DNA. From the absorption spectroscopy tests, K_b values of C3 were calculated as $2.8 \times 10^3 \text{ L}\cdot\text{mol}^{-1}$ ($r^2 = 0.996$). This value is similar to the reported values in the literature.^[41] It demonstrated the interaction between complex and DNA is relatively strong.

It shows the viscosity of DNA raises steadily with increasing the concentration of the complexes C3 and Ligand L3 in Figure 8. This may be explained by the complexes intercalating the adjacent DNA base pairs, and it leads an increase in the separation of base pairs at intercalation sites. Thus, the contour length of DNA was increased. The result is consistent with fluorescence studies. The interaction of C3 with calf thymus DNA was intercalation. So the results demonstrated that the C3 and L3 could bind to DNA by intercalation, but the order of the intensity of the action is $\text{C3} > \text{L3}$, it is consistent with the absorption spectroscopic studies.

Conclusion

Schiff base organotin (IV) complexes C1 ~ C3 have been synthesized. There are two independent dinuclear molecule in C1, the central tin atom is six-coordinate in distorted octahedron geometry. For C2, it exhibit a ladder structure. The C3 is a monomer structure, the central tin atom is five-coordinate in distorted trigonalbipyramid geometry. The

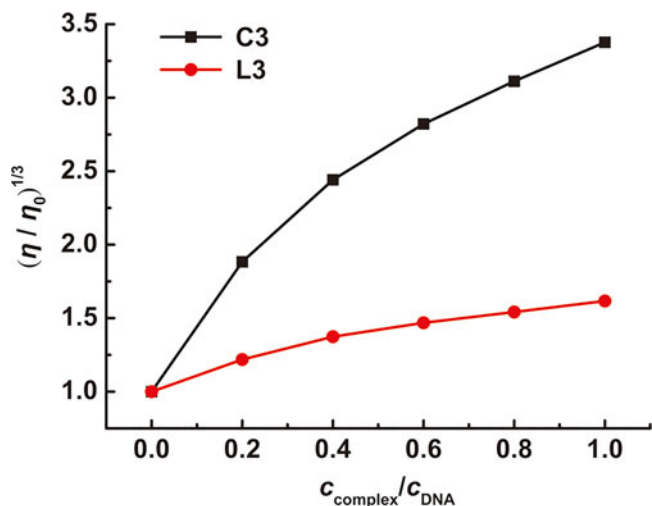


Figure 8. Effect of increasing amounts of the complex C3 and L3 on the relative viscosity at $25.0 \pm 0.1^\circ\text{C}$.

anticancer activity tests showed that C3 may be better potential candidates for further chemical optimization and cancer therapy. The interaction of C3 with calf thymus DNA was intercalation.

Funding

This work was supported by the Hunan Provincial Natural Science Foundation of China (Nos. 2017JJ3003, 2016JJ5004) and Foundation of Key Laboratory of Functional Metal-Organic Compounds of Hunan Province (No. MO18K01).

References

- Jimenez-Perez, V. M.; Garcia-Lopez, M. C.; Munoz-Flores, B. M.; Chan-Navarro, R.; Berrones-Reyes, J. C.; Dias, H. V. R.; Moggio, I.; Arias, E.; Serrano-Mireles, J. A.; Chavez-Reyes, A. New Application of Fluorescent Organotin Compounds Derived from Schiff Bases: Synthesis, X-ray Structures, Photophysical Properties, Cytotoxicity and Fluorescent Bioimaging. *J. Mater. Chem. B* **2015**, *3*, 5731–5745. DOI: [10.1039/C5TB00717H](https://doi.org/10.1039/C5TB00717H).
- Chandrasekhar, V.; Mohapatra, C. 2D-Coordination Polymer Containing Interconnected 82-Membered Organotin Macrocycles. *Cryst. Growth Des.* **2013**, *13*, 4655–4658. DOI: [10.1021/cg401363p](https://doi.org/10.1021/cg401363p).
- Rivera, J. M.; Reyes, H.; Cortés, A.; Santillan, R.; Lacroix, P. G.; Lepetit, C.; Nakatani, K.; Farfán, N. Second-Harmonic Generation within the P212121 Space Group, in a Series of Chiral (Salicylaldiminato)tin Schiff Base Complexes. *Chem. Mater.* **2006**, *18*, 1174–1183.
- Yin, H.; Hong, M.; Xu, H.; Gao, Z.; Li, G.; Wang, D. Self-Assembly of Organotin(IV) Moieties with the Schiff-Base Ligands Pyruvic Acid Isonicotinyl Hydrazone and Pyruvic Acid Salicylhydrazone: Synthesis, Characterization, and Crystal Structures of Monomeric or Polymeric Complexes. *Eur. J. Inorg. Chem.* **2005**, *2005*, 4572–4581. DOI: [10.1002/ejic.200500412](https://doi.org/10.1002/ejic.200500412).
- Hazra, S.; Paul, A.; Sharma, G.; Koch, B.; da Silva, M. F. C. G.; Pombeiro, A. J. L. Sulfonated Schiff Base Sn(IV) complexes as Potential Anticancer Agents. *J. Inorg. Biochem.* **2016**, *162*, 83–95.
- Hong, M.; Yin, H.; Zhang, X.; Li, C.; Yue, C.; Cheng, S. Di- and Tri-organotin(IV) complexes with 2-hydroxy-1-naphthaldehyde 5-chloro-2-hydroxybenzoylhydrazone: Synthesis, characterization and in Vitro Antitumor Activities. *J. Organomet. Chem.* **2013**, *724*, 23–31. DOI: [10.1016/j.jorganchem.2012.10.031](https://doi.org/10.1016/j.jorganchem.2012.10.031).
- Shujah, S.; Zia Ur, R.; Muhammad, N.; Ali, S.; Khalid, N.; Tahir, M. N. New Dimeric and Supramolecular Organotin(IV) complexes with a Tridentate Schiff Base as Potential Biocidal Agents. *J. Organomet. Chem.* **2011**, *696*, 2772–2781.
- Singh, R. V.; Chaudhary, P.; Chauhan, S.; Swami, M. Microwave-assisted Synthesis, characterization and Biological Activities of Organotin (IV) complexes with Some Thio Schiff Bases. *Spectrochim. Acta A* **2009**, *72*, 260–268. DOI: [10.1016/j.saa.2008.09.017](https://doi.org/10.1016/j.saa.2008.09.017).
- Lee, S. M.; Sim, K. S.; Lo, K. M. Synthesis, characterization and Biological Studies of Diorganotin(IV) complexes with Tris [(Hydroxymethyl)aminomethane] Schiff Bases. *Inorg. Chim. Acta* **2015**, *429*, 195–208. DOI: [10.1016/j.ica.2015.01.017](https://doi.org/10.1016/j.ica.2015.01.017).
- Rehman, W.; Haq, S.; Rahim, F.; Khan, S.; Waseem, M.; Nawaz, M.; Abid, O.-U.-R.; Qursehi, M. T.; Guo, C.-Y. Synthesis, Characterization and Antibacterial Screening of Diorganotin(IV) Complexes Derived from 2-[(4-Dimethylamino-Benzylidene) Amino] Phenol. *Pharm. Chem. J.* **2017**, *51*, 115–118.
- Cozzi, P. G. Metal-Salen Schiff Base Complexes in Catalysis: practical Aspects. *Chem. Soc. Rev.* **2004**, *33*, 410–421.
- Jiang, W. J.; Kuang, D. Z.; Feng, Y. L.; Yu, J. X.; Zhang, F. X.; Zhu, X. M. Microwave-Assisted Synthesis, Characterization and Fluorescence Properties of the Salicylaldehyde-o-aminophenol Schiff Base with Appended Donor Functionality and Their n-Butyltin(IV) Complexes. *Chin. J. Org. Chem.* **2014**, *34*, 2288–2295. DOI: [10.6023/cjoc201404037](https://doi.org/10.6023/cjoc201404037).
- Tan, Y.-X.; Zhang, Z.-J.; Liu, Y.; Yu, J.-X.; Zhu, X.-M.; Kuang, D.-Z.; Jiang, W.-J. Synthesis, crystal Structure and Biological Activity of the Schiff Base Organotin(IV) complexes Based on Salicylaldehyde-o-Aminophenol. *J. Mol. Struct.* **2017**, *1149*, 874–881. DOI: [10.1016/j.molstruc.2017.08.058](https://doi.org/10.1016/j.molstruc.2017.08.058).
- Tan, Y.; Zhang, Z.; Tan, Y.; Kuang, D.; Yu, J.; Zhu, X.; Jiang, W. Syntheses, crystal Structures and Biological Activity of the Dialkyltin Complexes Based on 2-oxo-3-phenylpropionic Acid Salicyloylhydrazone. *J. Coord. Chem.* **2017**, *70*, 2606–2624. DOI: [10.1080/00958972.2017.1355460](https://doi.org/10.1080/00958972.2017.1355460).
- Tan, Y.-X.; Zhang, Z.-J.; Feng, Y.-L.; Yu, J.-X.; Zhu, X.-M.; Zhang, F.-X.; Kuang, D.-Z.; Jiang, W.-J. Syntheses, Crystal Structures and Biological Activity of the 1D Chain Benzyltin Complexes Based on 2-Oxo-Propionic Acid Benzoyl Hydrazone. *J. Inorg. Organomet. Polym.* **2017**, *27*, 342–352. DOI: [10.1007/s10904-016-0477-5](https://doi.org/10.1007/s10904-016-0477-5).
- Zhang, Z. J.; Kuang, D. Z.; Jiang, W. J.; Yu, J. X.; Zhu, X. M.; Zhang, F. X. Synthesis, Crystal Structure, and Thermal Stability of a Dibutyltin Complex $\{[4\text{-Et}_2\text{NC}_6\text{H}_3(\text{O})\text{C}=\text{NC}_6\text{H}_3(\text{O})\text{-5-NO}_2](n\text{-Bu}_2\text{Sn})\}_2$ and Its Interaction with DNA. *Chinese J. Struct. Chem.* **2014**, *09*, 1319–1325.
- Jiang, W. J.; Wu, X. M.; Liu, C.; Yu, J. X.; Zhu, X. M.; Feng, Y. L.; Zhang, F. X.; Kuang, D. Z. Syntheses, Crystal Structures and Biological Activity of Schiff Base Organotin Complexes Based on o-Vanillin and 2-Amino-4-Nitrophenol. *Chinese J. Inorg. Chem.* **2015**, *07*, 1321–1328.
- Sheldrick, G. M. SHELXL-97. A Program for Crystal Structure Refinement, University of Göttingen, Germany, **1997**.
- Farrugia, L. J. WINGX: A Windows Program for Crystal Structure Analysis, University of Glasgow, Germany, **1988**.
- Pyle, A. M.; Rehmann, J. P.; Meshoyrer, R.; Kumar, C. V.; Turro, N. J.; Barton, J. K. Mixed-ligand Complexes of Ruthenium(II): Factors Governing Binding to DNA. *J. Am. Chem. Soc.* **1989**, *111*, 3051–3058. DOI: [10.1021/ja00190a046](https://doi.org/10.1021/ja00190a046).
- Tan, C.; Liu, J.; Chen, L.; Shi, S.; Ji, L. Synthesis, structural Characteristics, DNA Binding Properties and Cytotoxicity Studies of a Series of Ru(III) Complexes. *J. Inorg. Biochem.* **2008**, *102*, 1644–1653. DOI: [10.1016/j.jinorgbio.2008.03.005](https://doi.org/10.1016/j.jinorgbio.2008.03.005).
- Cinarli, A.; Gurbuz, D.; Tavman, A.; Birteksoz, A. S. Spectral Characterization and Antimicrobial Activity of Some Schiff Bases Derived from 4-Chloro-2-aminophenol and Various

- Salicylaldehyde Derivatives. *Chin. J. Chem.* **2012**, *30*, 449–459. DOI: [10.1002/cjoc.201180473](https://doi.org/10.1002/cjoc.201180473).
23. Yadav, S.; Yousuf, I.; Usman, M.; Ahmad, M.; Arjmand, F.; Tabassum, S. Synthesis and Spectroscopic Characterization of Diorganotin(IV) complexes of N [prime or Minute]- (4-hydroxy-pent-3-en-2-ylidene) isonicotinohydrazide: chemotherapeutic Potential Validation by in Vitro Interaction Studies with DNA/HSA, DFT, molecular Docking and Cytotoxic Activity. *RSC Adv.* **2015**, *5*, 50673–50690. DOI: [10.1039/C5RA06953J](https://doi.org/10.1039/C5RA06953J).
 24. Basu Baul, T. S.; Kehie, P.; Duthie, A.; Guchhait, N.; Raviprakash, N.; Mokhamatam, R. B.; Manna, S. K.; Armata, N.; Scopelliti, M.; Wang, R.; Englert, U. Synthesis, Photophysical Properties and Structures of Organotin-Schiff Bases Utilizing Aromatic Amino Acid from the Chiral Pool and Evaluation of the Biological Perspective of a Triphenyltin Compound. *J. Inorg. Biochem.* **2017**, *168*, 76–89. DOI: [10.1016/j.jinorgbio.2016.12.001](https://doi.org/10.1016/j.jinorgbio.2016.12.001).
 25. Yang, Y.; Hong, M.; Xu, L.; Cui, J.; Chang, G.; Li, D.; Li, C.-z. Organotin(IV) complexes Derived from Schiff Base N¹-[(1E)-(2-hydroxy-3-methoxyphenyl)methylidene] pyridine-3 -carbohydrazone: Synthesis, in Vitro Cytotoxicities and DNA/BSA Interaction. *J. Organomet. Chem.* **2016**, *804*, 48–58. DOI: [10.1016/j.jorganchem.2015.12.041](https://doi.org/10.1016/j.jorganchem.2015.12.041).
 26. Nath, M.; Saini, P. K.; Kumar, A. Synthesis, structural Characterization, biological Activity and Thermal Study of Tri- and Diorganotin(IV) complexes of Schiff Base Derived from 2-Aminomethylbenzimidazole. *Appl. Organometal. Chem.* **2009**, *23*, 434–445. DOI: [10.1002/aoc.1537](https://doi.org/10.1002/aoc.1537).
 27. Hong, M.; Chang, G.; Li, R.; Niu, M. Anti-proliferative Activity and DNA/BSA Interactions of Five Mono- or di-organotin(IV) compounds Derived from 2-hydroxy-N[prime or Minute]-[(2-hydroxy-3-methoxyphenyl)methylidene]-Benzohydrazone. *New J. Chem.* **2016**, *40*, 7889–7900. DOI: [10.1039/C6NJ00525J](https://doi.org/10.1039/C6NJ00525J).
 28. Pretsch, E.; Buhlmann, P.; Martin, B. *Structure Determination of Organic Compounds, Tables of Spectral Data*, 4th ed.; Springer-Verlag, Berlin Heidelberg, **2009**.
 29. Fulmer, G. R.; Miller, A. J. M.; Sherden, N. H.; Gottlieb, H. E.; Nudelman, A.; Stoltz, B. M.; Bercau, J. E.; Goldberg, K. I. NMR Chemical Shifts of Trace Impurities: Common Laboratory Solvents, Organics, and Gases in Deuterated Solvents Relevant to the Organometallic Chemist. *Organometallics* **2010**, *29*, 2176–2179. DOI: [10.1021/om100106e](https://doi.org/10.1021/om100106e).
 30. Arjmand, F.; Yousuf, I. Synthesis, characterization and in Vitro DNA Binding of Chromone Schiff Base Organotin(IV) Complexes. *J. Organomet. Chem.* **2013**, *743*, 55–62. DOI: [10.1016/j.jorganchem.2013.06.018](https://doi.org/10.1016/j.jorganchem.2013.06.018).
 31. Nath, M.; Saini, P. K. Chemistry and Applications of Organotin(IV) Complexes of Schiff Bases. *Dalton Trans.* **2011**, *42*, 7077. DOI: [10.1039/c0dt01426e](https://doi.org/10.1039/c0dt01426e).
 32. Basu, S.; Masharing, C.; Das, B. Diorganotin(IV) complexes of Polyaromaticazo-azomethine Ligand Derived from Salicylaldehyde and Ortho-aminophenol: Synthesis, Characterization, and Molecular Structures. *Heteroatom Chem.* **2012**, *23*, 457–465. DOI: [10.1002/hc.21037](https://doi.org/10.1002/hc.21037).
 33. Chandrasekhar, V.; Gopal, K.; Sasikumar, P.; Thirumoorthi, R. Organotin(IV) Assemblies from Sn-C Bond Cleavage Reactions. *Coord. Chem. Rev.* **2005**, *249*, 1745–1765. DOI: [10.1016/j.ccr.2005.03.028](https://doi.org/10.1016/j.ccr.2005.03.028).
 34. Beltrán, H. I.; Damian-Zea, C.; Hernández-Ortega, S.; Nieto-Camacho, A.; RamíRez-Apan, M. T. Synthesis and Characterization of di-phenyl-tin(IV)-salicyliden-ortho-aminophenols: Analysis of in Vitro Antitumor/antioxidant Activities and Molecular Structures. *J. Inorg. Biochem.* **2007**, *101*, 1070–1085. DOI: [10.1016/j.jinorgbio.2007.04.002](https://doi.org/10.1016/j.jinorgbio.2007.04.002).
 35. Çelebier, M.; Şahin, E.; Ancin, N.; Öztaş, N. A.; Öztaş, S. G. Synthesis and Characterization of Diorganotin(IV) complexes of Schiff Bases with ONO-type Donors and Crystal Structure of [N-(2-hydroxy-4-nitrophenyl)-3-ethoxysalicylideneiminato] diphenyltin(IV). *Appl. Organometal. Chem.* **2007**, *21*, 913–918.
 36. Asadi, Z.; Asadi, M.; Setoodehkhah, M. Thermodynamics of Adduct Formation of Cobalt(II) tetraaza Schiff Base Complexes with Organotin(IV) Trichlorides. *Spectrochim. Acta A Mol. Biomol. Spectrosc.* **2013**, *112*, 214–218.
 37. Chang, J. H.; Dong, Q. G. *Spectral Theory and Analysis*; Science Press, Beijing, **2012**.
 38. Zhao, G.; Shi, X.; J. Liu, J. Z.; Xiao, H.; L. Synthesis, S. Crystal Structures and Biological Activity of Transition Metalcomplexes of 2-phenyl-4-selenazole Carboxylic Acid. *Sci. China Chem.* **2010**, *40*, 1525–1534.
 39. Xu, J. G.; Wang, Z. B. *Fluorescence Analysis*, 3rd ed.; Science Press, Beijing, **2006**.
 40. Yan, C.; Zhang, J.; Liang, T.; Li, Q. Diorganotin (IV) complexes with 4-nitro-N-phthaloyl-glycine: Synthesis, characterization, antitumor Activity and DNA-binding Studies. *Biomed. Pharmacother.* **2015**, *71*, 119–127. DOI: [10.1016/j.biopha.2015.02.027](https://doi.org/10.1016/j.biopha.2015.02.027).
 41. Hussain, S.; Ali, S.; Shahzadi, S.; Tahir, M. N.; Shahid, M. Synthesis, characterization, biological Activities, Crystal Structure and DNA Binding of Organotin(IV) 5-Chlorosalicylates. *J. Coord. Chem.* **2015**, *68*, 2369–2387. DOI: [10.1080/00958972.2015.1046849](https://doi.org/10.1080/00958972.2015.1046849).